

A Potential Pozzolanic Material consisting of Rice Straw Ash and Fly Ash for Geopolymer Mortar Production-based Cementitious System

A. Arwin Amiruddin

Department of Civil Engineering, Hasanuddin University, Makassar, Indonesia
a.arwinamiruddin@yahoo.com (corresponding author)

M. Tumpu

Disaster Management Study Program, Graduate School, Hasanuddin University, Indonesia
tumpumiswar@gmail.com

Parea R. Rangan

Department of Civil Engineering, Christian University of Indonesia, Toraja, Indonesia
pareausanrangan68@gmail.com

Rita Irmawaty

Department of Civil Engineering, Hasanuddin University, Makassar, Indonesia
rita_irmawaty@yahoo.co.id

Bambang Bakri

Department of Civil Engineering, Hasanuddin University, Makassar, Indonesia
bambangbakri@gmail.com

Mansyur

Department of Civil Engineering, Sembilanbelas November University, Kolaka, Indonesia
mansyurusn14@gmail.com

Received: 12 August 2024 | Revised: 6 September 2024 | Accepted: 22 September 2024

Licensed under a CC-BY 4.0 license | Copyright (c) by the authors | DOI: <https://doi.org/10.48084/etasr.8703>

ABSTRACT

Rice straw waste, among other issues, is a significant source of air pollution and methane emissions from biological decomposition. This study examines the use of Rice Straw Ash (RSA), when combined with Fly Ash (FA) and Laterite Soil (LS), as a pozzolan in cementitious systems. The study's purpose is to examine the microstructure and compressive strength of a geopolymer mortar composed of FA, RSA, and LS. The RSA is activated with sodium hydroxide (NaOH), an alkaline activator, with concentrations of 6, 12, and 15 M NaOH. After air and water curing for 3, 7, and 28 days, the compression strength of the geopolymer mortar was tested. To determine the dominant compound of the pozzolan reactions that were generated in cementitious systems, Scanning Electron Microscopy (SEM) and X-Ray Diffraction (XRD) were employed. When geopolymer mortar is cured in air and water, its compressive strength increases with age. This is due to the fact that RSA, FA, and LS have the ability to form iron oxide (Fe_3O_4) in the amorphous phase and have a strong bond with alumina (Al_2O_3) and silica (SiO_2). The material's fineness affects its compressive strength as well. This study intends to replace cement in mortar and concrete utilizing environmentally friendly materials. Furthermore, the creation of geopolymer material usually requires the use of oven heat to enhance the geopolymerization procedure. However, this study shows that this method does not require oven heat.

Keywords-pozzolanic material; rice straw ash; geopolymer mortar; cementitious systems

I. INTRODUCTION

The global market for Portland cement concrete is expanding at an exponential rate. Due to the continuous expansion of infrastructure, more concrete and mortar are needed for construction projects [1, 2]. Environmental issues including the discharge of carbon dioxide (CO₂) gas are brought on by this growth [3]. Coal is a common source for power plants. One consequence of burning coal that is classified as a pollution source, is Fly Ash (FA) [4].

People perceive cement as a substance that is "less friendly" to the environment since burning cement-based materials demands temperatures as high as 1500°C [5, 6]. This is predicated on the notion that the emissions of CO₂ produced equal the volume of the cement itself. Due to its critical role in the process of global warming, CO₂ is commonly referred to as a greenhouse gas [5, 7]. One of the main sources of emissions in Indonesia and other nations is the production of cement. Cement manufacturing is essential to the industrial decarbonization in underdeveloped countries [6, 8]. Air, water, auxiliary materials, fuel (such as petroleum coke, coal, natural gas, fuel oil, biomass, or some waste), energy (such as electricity and heat), and raw materials are all extensively used in the complicated process of creating cement. The environment is severely harmed by the usage and processing of these raw resources. During the calcination process, the decarbonization of limestone releases around half of the CO₂ created during cement manufacturing [9–14]. By passing the Law of the Republic of Indonesia Number 17 of 2004, Indonesia affirmed its adherence to the Kyoto Protocol to the United Nations Framework Convention on Climate Change (UNFCCC) [15].

When aggregate and cement are mixed to make mortar or concrete, the cement acts as a binder. To make mortar and concrete, cement frequently acts as a glue between coarse and fine particles. Because cement is made of non-renewable materials, it depletes natural resources. The creation of geopolymers is one initiative aimed at lowering cement consumption. Numerous studies have demonstrated that geopolymer binders can be used to create mortar or concrete, and that the physical characteristics of mortar or concrete formed from materials containing pozzolan are identical to those of mortar or concrete made from cement. Geopolymers can be produced by certain minerals that contain pozzolan. These materials are FA, straw ash, and Laterite Soil (LS). These three materials are considered waste. One of the consequences of burning coal in steam power plants is FA. Research on the use of geopolymer-based polymers as material binder to create environmentally friendly products has been prompted by the significant amounts of CO₂ that cement manufacturing releases into the atmosphere during the production of cement. FA, LS, and Rice Straw Ash (RSA) have significant silica and alumina contents. The silica and alumina found in RSA, FA, and LS can be mixed with alkaline liquids to form binders.

Alkaline activators include sodium hydroxide (NaOH) and sodium silicate (Na₂SiO₃) [16]. NaOH interacts with the silicon and aluminium in FA to facilitate the formation of strong polymer linkages, whereas Na₂SiO₃ quickens the

polymerization reaction. The concentration and amount of the alkaline activator, in addition to NaOH and Na₂SiO₃ activators, also influence the FA geopolymer bond strength. Aluminosilicate networks, which can be crystalline or amorphous, are created when the solid and activator components are combined, initiating the hardening process. Na₂SiO₃ deforms the geopolymer because it functions as an alkali activator either when used alone or in conjunction with NaOH. NaOH was used as an alkaline activator in this investigation.

The ozone layer depletion and the urgent issue of global warming have made it necessary for the construction industry to employ more environmentally friendly building materials. Because it is lucrative to use waste from byproducts to replace cement and reduce greenhouse gas emissions, researchers and construction professionals are starting to pay attention to geopolymer materials. They have superior mechanical properties and are more durable than conventional concrete. Although geopolymer materials are inexpensive, there is currently relatively little research on their structural, design, and application features, which limits their practical utility. The results of earlier research show that geopolymer concrete can take the place of traditional concrete. Authors in [19] discovered that FA-based geopolymer concrete strengthened more quickly in the presence of a high concentration of NaOH after being exposed to seawater for three years. Moreover, the geopolymer concrete's chloride Diffusion Coefficient (DC) and steel corrosion decreased as the mixture's NaOH concentration rose. As the amount of NaOH increases, the amount of chlorine that can be added to geopolymer concrete reduces as a proportion of the total chloride content. The impact of hydrocarbon fire exposure on the compressive strength characteristics of geopolymer concrete panels and cylinders was examined in [20]. The components are FA, 0.3% absorption sand, and coarse aggregate (maximum 14 mm diameter basalt). Sodium silica in an 8 M NaOH solution (SiO₂:Na₂O = 2) was the material used to make both the salty sand and the large pieces in SSD. The results showed that the samples exhibited little spalling and that mass losses ranging from 2.70 to 4.65 were caused by moisture loss during heating. The spalling resistance of geopolymer concrete is better than that of Ordinary Portland Cement (OPC). This is caused by the aggregate's and geopolymer paste's low differential gradient and thermal incompatibility. Authors in [21] showed that geopolymer concrete can achieve the strength required for structural design; nevertheless, the material's compressive strength and flexural tensile strength are affected by the curing process, which causes surface shrinkage. The experiments showed that, with little parameter tweaks, AEMM can accurately calculate the long-term deflection of geopolymer concrete blocks. Authors in [22] looked into the durability of FA-based geopolymer concrete with added calcium. The resistance to sulfuric acid was assessed by the researchers after 28, 90, and 365 days. Stone fragments up to 12.5 mm in diameter, a specific gravity of 2.75, and 1% water absorption were the materials employed, along with a NaOH concentration of 10 M, a Na₂SiO₃ to NaOH ratio of 2.5, and FA with a specific gravity of 2.36. Furthermore, they employed river sand, with a specific gravity of 2.54, a fineness modulus of

2.51, and a water absorption of 0.2%, as fine aggregate. Compressive strength decreases with increasing alkali activator/FA solution ratios and recycled material volume [23]. The poor compressive strength value of the recycled material can be attributed to its porosity and liquid impact. For maximum compressive strength, 40 °C is the optimal treatment temperature and 10 M is the ideal concentration of NaOH. Authors in [24] state that the compressive strength value may rise depending on the concentration of NaOH used as an alkaline activator solution. Compressive strength of up to 47 MPa can be obtained by the 1:1 ratio of NaOH to Na_2SiO_3 and the activation of the geopolymer towards FA. This figure, which exceeds the concrete compressive strength criterion of 40 MPa, demonstrates the potential of FA as a cement alternative. Authors in [25] examined the performance of low calcium FA combined with coarse aggregate floating steel slag (SFS) in geopolymer concrete (GPC).

The evaluated geopolymer material has a somewhat low thermal stability rating [26]. The samples using salt as the activator exhibited a significant decrease in strength at 800 °C. At 1000 °C, the compressive strength of materials made with potassium silicate and FA begins to decrease, despite a significant rise upon heating. When compacted at 1–10 MPa, combustion shrinkage is reduced for all materials. Compressive strength variations and shrinkage are observed in materials composed of geopolymers using class F FA and an alkaline activator. When the temperature climbs between 800–1200°C, certain changes take place. As a result, it was decided that the material was inappropriate for uses requiring insulation that is fire-resistant. The use of Ground Granulated Blast Furnace Slag (GGBS) and Palm Oil Fuel Ash (POFA) as binders and Oil Palm Shell (OPS) as coarse aggregate is a novel approach to building using concrete. Authors in [27] produced lightweight geopolymer concrete. The effects of various aggregates, such as mine sand (NS), production sand (MS), and quartz dust (QD), were examined and reported while variables like water and activator content were kept constant. The NaOH concentration used was 12 M, with a constant ratio of $\text{Na}_2\text{SiO}_3/\text{NaOH} = 2.5$. The results show that lightweight concrete based on OPS and containing 425 kg/m^3 of binder yields the highest compressive strength of 33 MPa. The research indicates that compared to ordinary concrete, OPS geopolymer concrete has a 50–60% smaller carbon footprint.

Recycling construction waste and other discarded materials into pavement blocks can address sustainability issues like resource conservation and converting byproducts into valuable and usable goods. Alkali activators are created during carbonate calcination, and this undoubtedly increases atmospheric CO_2 levels. Consequently, the CO_2 footprint of geopolymer concrete blocks is influenced by the kind, potency, and dosage of the alkali activator [28]. Pozzolanic materials—either naturally occurring or synthesized—are the main ingredient in geopolymer paste. Alumina and silica-containing pozzolan minerals can be used as binder materials. Among these are FA, metakaolin, husk ash, RSA, LS, and volcanic materials [29]. For the creation of geopolymer mortar, an activator, such as potassium or sodium hydroxide, and a material source abundant in silica (Si) and aluminium (Al) are

required since they speed up the critical chemical reactions [30].

Several studies indicate that when utilizing FA geopolymer as a material binder instead of cement, heat from an oven is always needed to develop and increase the strength of concrete. Therefore, in order to transform FA, LS, and RSA into concrete or geopolymer mortar, oven heat is needed. Semiquantitative testing is another option for assessing geopolymer blends in addition to the usual empirical tests. Testing using X-Ray Diffraction (XRD) is one such method. To ascertain the elements, compounds, phases, and crystal structures that are present on a qualitative level, we perform XRD testing. Atoms effectively arrange themselves into a crystal structure, and diffraction-based experimental techniques study the micro/phase structure. The form of the unit cell can be ascertained by analysing the diffraction pattern produced by the passage of waves in crystal structures and compounds [17, 18]. In this work, we employ FA, RSA, and LS bound with NaOH as an alkaline activator in water curing and air curing to examine the microstructure using XRD testing and the mechanical properties using compressive strength tests after 3, 7, and 28 days of curing. This study is distinctive in that the silica and alumina in the materials were activated without the application of oven heat.

II. MATERIALS AND METHODS

A. Materials

The physical characteristics of the RSA employed in this investigation are shown in Table I. Tests were conducted on the physical characteristics of RSA using the SNI (Indonesian National Standards) criteria. RSA was made in the South Sulawesi Province's Tana Toraja Regency by burning rice harvesting waste at a temperature of roughly 900 °C.

TABLE I. PHYSICAL PROPERTIES OF RSA

No.	Checking types	Standard tests	Check-up results
1	Specific gravity	SNI 03-1964-2008	2.41
2	Water absorption	SNI 1970:2008	62.10%

TABLE II. RSA SIEVE ANALYSIS TEST RESULTS

No. Filter	Retained weight (g)	Total retained weight (g)	Percent total	
			Retained	Passed
50	0	0	0	100.00
100	188.75	188.75	94.37	5.62
200	10.10	198.85	99.42	0.57
325	1.05	199.90	99.95	0.05
Pan	0.10	200.00	100.00	0.00

The findings of the RSA filter analysis are shown in Table II. It is evident that filter number 200 efficiently holds onto over 90% of the RSA. Table III presents the results of evaluating the chemical characteristics of RSA based on the results of the XRF test. At 71.50%, silica compounds (SiO_2) make up the majority of the content of RSA. Other important constituents include Fe_2O_3 , Cl, P_2O_5 , K_2O , and CaO. Reading the small compounds from the straw ash, we were able to identify MnO, TiO_2 , Rb_2O , ZnO, SrO, Nb_2O_5 , and MoO_3 . By establishing bonds with other materials, we expect the silica in the straw ash to solidify inside the geopolymer mortar.

TABLE III. CHEMICAL PROPERTIES OF RSA (XRF TEST)

No.	Oxide compounds	Content (%)
1	SiO ₂	71.50
2	K ₂ O	16.98
3	CaO	6.43
4	P ₂ O ₅	4.16
5	Fe ₂ O ₃	3.13
6	Cl	2.54
7	MnO	0.113
8	TiO ₂	0.302
9	Rb ₂ O	0.0382
10	ZnO	0.0120
11	SrO	0.0086
12	Nb ₂ O ₅	0.0016
13	MoO ₃	0.0035

The properties of FA which came from trash produced by the steam power plant in Jeneponto Regency and Punagayya Village, South Sulawesi Province, are listed in Tables IV-V. FA has a specific gravity of 2.41, higher than that of RSA and LS, according to the specific gravity analysis in Table IV. The greater specific gravity of FA can be attributed to its fine grain size, which according to ACI Committee 226 criteria passes through filter No. 200 with over 90% and sieve No. 325 (45 millimetres) with 5-27%. Furthermore, Table V displays the chemical characteristics of FA as ascertained by the XRD test outcomes. FA is divided into three classes by ASTM C 618-03: class N, F, and C. The minimal percentage of SiO₂, Al₂O₃, and Fe₂O₃ components in both class N and F FA is 70%. Class C FA, on the other hand, has a composition that ranges from 50% to 70%. FA in classes N and F usually has a much lower CaO content than that in class C, where the CaO level is around 10% [31]. The CaO element is present in less than 20% of FA in class F. The fly ash used in this study is categorized as type F FA, or low calcium FA [32, 33]. Compared to other types of FA, the Jeneponto FA employed in this study has a CaO level of 14.12%, which can cause a twofold reaction and reduce setting time. Jeneponto FA has pozzolanic characteristics; cementitious properties can only be produced by adding quick lime, hydrated lime, or cement. In the first step, calcium combines with water to produce a reaction known as lime-induced hydration. The second process, the geopolymerization of silica and alumina, is triggered by alkali.

TABLE IV. RESULTS OF INSPECTION OF FA CHARACTERISTICS

No.	Material characteristics	Result
1	Specific gravity	2.99
2	Sieve analysis	> 90% passed No. 200

TABLE V. CHEMICAL PROPERTIES OF FA (XRF TEST)

Compound	SiO ₂	Al ₂ O ₃	Fe ₂ O ₃	CaO	MgO	K ₂ O	Na ₂ O
Content (%)	45.96	14.81	11.37	15.15	3.87	0.81	0.53

The findings of the assessment of the physical properties of LS are shown in Table VI. LS was obtained from the University of Christian Indonesia Toraja. After extracting the soil, we tested it using a sieve analysis test. If the soil passes sieve No. 200 (0.075 mm) with percentage better than 89.00%, it can be classified into groups A-4, A-5, A-6, and A-7. The utilized LS belongs to group A-7-5 since it is a clay soil with high plasticity. Table VII presents an evaluation of the laterite

soil's chemical characteristics based on the findings of the XRF test. SiO₂, Fe₂O₃, Al₂O₃, TiO₂, K₂O, and Cl make up the majority of the LS in this study, making up 45.96, 11.37, 14.81, and 3.87, respectively.

LS contains large amounts of sesquioxide. Sesquioxide is composed of iron (Fe), aluminium (Al), and oxide and hydroxide components. LS has a brick-red to brownish tint due to the presence of Fe and Al, and a reddish-rust-coloured due to a high concentration of iron oxide (FeO). In LS, we can find a variety of sesquioxide minerals including the metals Fe, Al, Mn, and Ti. According to XRF data, the elements Ti and Al form minerals in the anatase and rutile mineral groups and the boehmite or diaspora mineral groups, respectively. Laterites usually contain large amounts of quartz and oxides. Materials like zircon, titanium (TiO), iron (Fe), tin (Ti), aluminium (Al), and manganese (Mn) are what are left over after extensive wear. The mineral and chemical makeup of LS is mostly determined by the parent rock or constituent stones. However, the condition of the soil and its components are greatly influenced by depth, climate, and location.

TABLE VI. PHYSICAL CHARACTERISTICS OF LS

Checking type		Checkup result	
		Result	Unit
Testing the physical properties of soft soil:			
Initial water content (w)		33.30	%
Specific gravity (Gs)		2.76	-
Sieve analysis and hydrometer inspection			
a	Sand	15.69	%
b	Silt	46.79	%
c	Clay	39.35	%
Atterberg Limits			
a	Liquid limit (LL)	46.20	%
b	Plastic limit (PL)	31.39	%
c	Plastic index (PI)	15.89	%
Standard compaction			
a	Maximum dry density, (γ _d)	15.27	kN/m ²
b	Optimum Moisture Content (OMC)	27.79	%
Classification based on USCS: ML, AASHTO: A-7-5			
Mechanical property testing of soft soil			
California Bearing Ratio – Unsoaked (CBR)		9.35	%

In its physical form, NaOH is represented as flat, solid flakes with a strong, stinging smell. It also appears to be brilliant white. The chemical composition of the NaOH component parts is shown in Table VII. The percentage composition of the NaOH compound is greater than 99%.

The XRF analysis's findings indicated that either the chemical compound NaOH was missing or the XRF instrument was unable to disassemble its parts. This is a result of the XRF equipment's inability to detect the minuscule energy that NaOH generates. The very low energy suggests that NaOH solution is made entirely of NaOH and contains no other materials.

TABLE VII. CHEMICAL COMPOSITION OF NAOH

No.	Chemical compounds	Composition (%)
1	NaOH	≥ 99.0
2	Na ₂ CO ₃	≤ 0.80
3	NaCl	≤ 0.10
4	Iron (Fe) ppm	≤ 50

B. Mix Design Geopolymer Mortar

Table VIII displays the geopolymer mortar mixture design. It has a volume of 1 m³ and is composed of LS, FA, RSA, and NaOH. FA made up 41.60% of the mixture. The ratio of FA, LS, and RSA is 41.66: 16.66: 41.66. The composition design of the geopolymer mortar was developed as a result of the preliminary mixing tests conducted under ideal conditions. NaOH solution was employed as an alkaline-binding agent. The amount of water used is considered in order to calculate the ideal water content for appropriate LS compaction. The molarity concentrations of the NaOH utilized in this investigation were 6, 12, and 15 M. Obviously, the quantity of NaOH used increases with the concentration of NaOH. The proportion of alkali to total materials is 7.98, 14.77, and 17.82 at 6, 12, and 15 M, respectively. The largest alkali-to-total material ratio is found at 15 M. The molarity determines how imperfect the geopolymerization reaction is. Sodium carbonate efflorescence (NaOH + CO₂ sodium carbonate) is a sign of this. The effluent's voids cause the geopolymer mortar's compressive strength to decline.

TABLE VIII. MIX DESIGN GEOPOLYMER MORTAR AT 15 M (1 m³)

No.	Material	Molarity/Total (kg)		
		6 M	12 M	15 M
1	Straw ash	60.392	60.392	60.392
2	Fly ash	150.979	150.979	150.979
3	Laterite soil	10.979	10.979	10.979
4	NaOH	30.196	60.392	75.490
5	Water	125.690	125.690	125.690

C. Research Design

The LS, FA, RSA, and alkaline activator required to make geopolymer mortar were provided by the province of South Sulawesi. We assessed and measured the compressive strength and chemical component composition by XRD. FA takes the place of cement in the composition of the geopolymer mortar mix. In order to activate the FA, the combination also contains water, RSA, LS, and NaOH. The concentrations of the NaOH solution that was employed were 6, 12, and 15 M. We used both air and water to dry the geopolymer mortar.

D. Sample Preparation

This study investigated the effects of age on geopolymer mortar using cylindrical moulds of 5 × 10 cm. The following mixing strategy was utilized in the research:

1. The materials were assembled according to the specifications.
2. LS, RSA, and FA were combined in the mixing bowl.
3. A mixer at low speed was used to blend the LS, FA, and RSA for 60 s. Then, manual stirring was employed until the mixture was thoroughly combined.
4. The NaOH, previously dissolved in water, was added while mixing the LS, FA, and RSA. Mixing was conducted at a slow pace for 1 min.

5. The mixture was stirred manually to ensure even distribution. Next, a mixer at high speed was used to blend the mixture for 1 min.
6. Using a tamping rod, the resulting slurry was print onto a mold in three layers, with each layer printed 25 times.
7. The mixture was allowed to solidify in the mold for 24 h.
8. The test object was removed from the mold, and air and water curing took place for 3, 7, and 28 days.
9. Finally, tests for compressive strength and chemical component composition (XRD) were conducted.

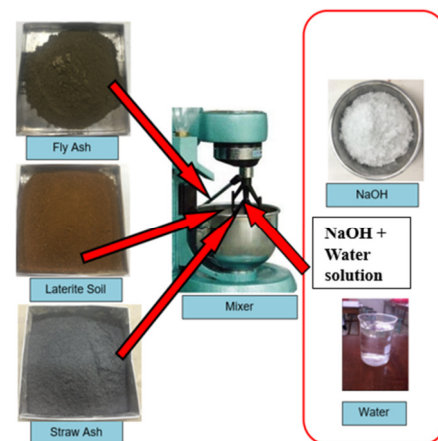


Fig. 1. Mixing geopolymer materials.

E. Compressive Strength Test

Compressive strength testing involves delivering a monotonous load to the test item continuously and at a constant rate, which puts the laden test object under compressive stress (SNI-03-6825-2002; SNI 1974-2011). When assessing compressive strength, a cylindrical test object is positioned standing or upright. When the test object is subjected to compressive stress, it eventually collapses or is destroyed [31, 32]. The test object's location for the compressive strength test of the geopolymer cylindrical mortar is shown in Figure 2. The test measures the displacement caused by the applied force in both the horizontal and vertical axes using an LVDT.

F. X-Ray Diffraction (XRD) Test

The interaction of the test sample with X-rays produces diffraction patterns in XRD. These patterns are produced and recorded by an X-ray apparatus. We can ascertain the structure of polymers, including their amorphous and crystalline phases, using XRD. Both crystalline and amorphous zones can haphazardly coexist in polymers. In their X-ray diffractograms, crystalline polymers have sharp peaks, whereas amorphous polymers usually show larger peaks.

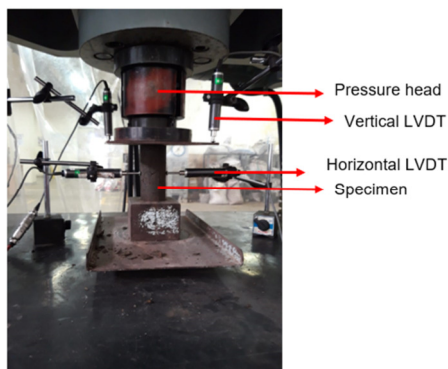


Fig. 2. Compressive strength test.

III. RESULTS AND DISCUSSION

A. Behavior of Geopolymer Mortar at Fresh Conditions

Figures 3-5 present the findings from flow tests conducted on a mixture of geopolymer mortar containing 6 M, 12 M, and 15 M concentrations. The behavior of fresh geopolymer mortar is shown in these figures. Using a 5% molarity, we found that fresh geopolymer mortar flows at the same rate of 112.50 mm at each molarity concentration, simulating the usual flow of mortar under fresh conditions [10–14]. In addition, the geopolymer mortar has a newly determined specific gravity of 1901.3 kg/m³. Due to the ability of this geopolymer mortar mixture to bond LS, fresh geopolymer mortar can flow and spread evenly without clumping or building up in the circle's centre.



Fig. 3. Flow of geopolymer mortar at 6 M concentration.



Fig. 4. Flow of geopolymer mortar at 12 M concentration.

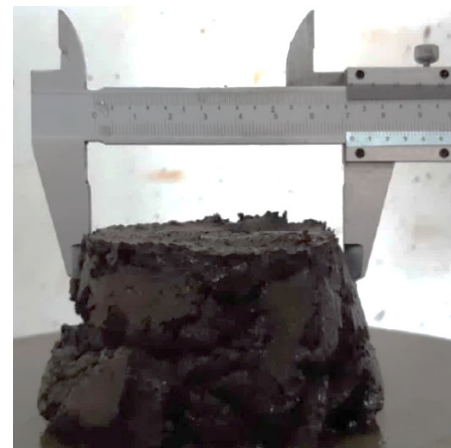


Fig. 5. Flow of geopolymer mortar at 15 M concentration.

B. Compressive Strength Test

Based on the outcomes of compressive strength tests performed after 3, 7, and 28 days, we were able to identify the ideal molar content of NaOH for both air and water curing. The compressive strength test results for geopolymer mortar composed of FA, RSA, and LS under typical air and water curing conditions are summarized in Table IX. Specimens with 6 M water and air curing yielded stress values of 0.460 N/mm² and 0.570 N/mm², after 3 days, 1.208 N/mm² and 1.287 N/mm², after 7 days, and 2.210 N/mm² and 2.241 N/mm² after 28 days, respectively.

In 12 M water- and air-cured specimens, the stress values were 1.287 N/mm² and 1.684 N/mm² after 3 days, 1.475 N/mm² and 1.721 N/mm² after 7 days, and 3.296 N/mm² and 3.209 N/mm² after 28 days, respectively. The stress values in the specimens that had been cured in 15 M water and in 15 M air were 0.589 N/mm² and 0.806 N/mm², after 3 days, 1.541 N/mm² and 1.692 N/mm² after 7 days, and 2.341 N/mm² and 2.443 N/mm² after 28 days, respectively.

The compressive strength values of geopolymer cement are shown in Figure 6 for all test item types under standard conditions. Both the compressive strength value and the molarity concentration employed increased with the age of the mortar. The test specimens' compressive strengths increased from 6 M (6MCA) to 12 M (12MCA) and 15 M (15MCA), or 64.26% and 21.91%, respectively, after 3 days of water curing. At 7 days old, the compressive strength values rose by 18.10% and 21.61%, respectively. The increases in compressive strength values at 28 days of age were 30.17% and 4.28%, respectively.

The compressive strength values increased from 6 M (6MCU) to 12 M (12MCU) and 15 M (15MCU) in air-cured test specimens that were 3 days old, or 66.16% and 29.29%, respectively. At 7 days of age, the increases in compressive strength values were 25.22% and 23.94%, respectively. The compressive strength values increased by 32.95% and 9.54%, respectively, at 28 days of age.

The age of the mortar has also an effect on the compressive strength rating. In particular, at from 3 to 7 and from 7 to 28 days of age, the compressive strength of water cured specimens

improved by 61.93% and 79.48%, respectively, at a concentration of 6 M. The compressive strength values rose by 55.72% and 74.21%, respectively, at a concentration of 6 M air curing. The compressive strength values rose to 2.15% and 48.91%, respectively, at a concentration of 12 M. The compressive strength values rose to 52.37% and 67.01%, respectively, at a concentration of 15 M.

Based on the results of compressive strength tests conducted at three molarity concentrations (6, 12, and 15 M), and air and water curing, we can infer that 12 M is the best molarity concentration since it gives the best compressive strength values.

It appears that the stress caused by the compressive load increases with age. This behavior is comparable to that of ordinary mortar. Furthermore, the study's use of LS, a fine aggregate material high in silica and alumina, influences this behavior. This substance, when mixed with FA and RSA, generates strong geopolymer linkages.

LS, with a liquid limit (LL) of 46.20%, can react with an alkaline activator to generate geopolymerization linkages. This reaction causes the geopolymer components to solidify and form strong connections, ensuring that the resulting pores are not too large or small. This produces a relatively high compressive strength rating. This is absolutely consistent with the results of XRD and SEM (microstructure) experiments performed on dominating chemicals, specifically silica and alumina.

[14–16]. The geopolymer material's hardness rating is not greatly affected by this union. The low molarity concentration of the alkaline activator (NaOH) can be the reason for its inability to properly bind the geopolymer substance. Layers, clusters, and long forms are seen in several geopolymer particles [6, 7].

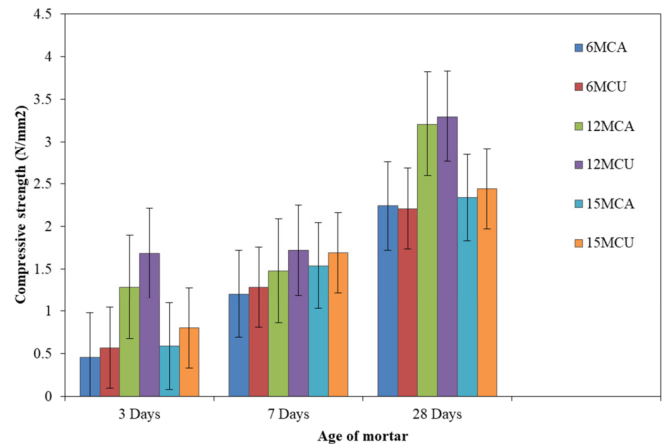


Fig. 6. Compressive strength value of geopolymer mortar

TABLE IX. RECAPITULATION OF COMPRESSIVE STRENGTH TEST RESULTS OF GEOPOLYMER MORTAR

Type variation	Curing	Age (days)	Peak stress-strain relationship (average)		
			Stress	Vertical strain	Horizontal strain
			(N/mm ²)	(mm/mm)	(mm/mm)
6 M (6MCA)	Water	3	0.460	0.0156	-0.00205
		7	1.208	0.0165	-0.00128
		28	2.241	0.0233	-0.00157
6 M (6MCU)	Air	3	0.570	0.0164	-0.00220
		7	1.287	0.0190	-0.00178
		28	2.210	0.0244	-0.00632
12 M (12MCA)	Water	3	1.287	0.0181	-0.00205
		7	1.475	0.0156	-0.00129
		28	3.209	0.0230	-0.00158
12 M (12MCU)	Air	3	1.684	0.0157	-0.0022
		7	1.721	0.0190	-0.0017
		28	3.296	0.0209	-0.0065
15 M (15MCA)	Water	3	0.589	0.0157	-0.0141
		7	1.541	0.0120	-0.00203
		28	2.341	0.0202	-0.00161
15 M (15MCU)	Air	3	0.806	0.0167	-0.00172
		7	1.692	0.0107	-0.00132
		28	2.443	0.0181	-0.00157

It is evident that test specimens cured by air had higher compressive strengths than specimens treated by water. This is due to the fact that the polymerization reaction progresses flawlessly in the air-cured test object as opposed to the water-cured test object [1, 9, 10, 33]. The combination of geopolymer components, such as FA, RSA, and LS, as well as the optimal polymerization process influence the test's density and hardness

The presence of material passing through sieve no. 200 is one of the elements influencing the qualities of geopolymer mortar, including compressive strength [5]. The durability of mortar is intimately correlated with its physical properties. Durability is determined by internal and exterior damage to the mortar itself [12]. A multitude of pore distribution characteristics are frequently present in mortar, which may have an impact on the mortar's absorption, diffusion, and sorptivity transport qualities.

C. X-Ray Diffraction (XRD) and Scanning Electron Microscopy (SEM) Test

After 28 days, the microstructure of the air-cured 6 M geopolymer mortar is shown in Figure 7. It is evident that the components that constitute the geopolymer combine well with the specimen's 6 M air cure microstructure. The geopolymer material's hardness rating is not greatly affected by this union. The low molarity concentration of the alkaline activator (NaOH) can be the reason for its inability to properly bind the geopolymer substance. Some geopolymer particles are long-shaped, grouped, and have layers. Figure 8 shows the microstructure of a 12 M geopolymer mortar test specimen that has been air-cured for 28 days, based on SEM observations. The microstructure of a test specimen for a 15 M straw ash geopolymer mortar that has been air-cured for 28 days is shown in Figure 9. The geopolymer mortar specimen displays ordered atomic structure crystallization, as can be seen. To make geopolymer mortar, combine straw ash, fly cremains, and laterite soil activated with NaOH. The components should blend well, solidify, and have a good density. The geopolymer mortar test object's compressive strength test reveals that the test object is even more resilient due to the existence of micro-visible crystallization. This is explained by the fact that crystallization significantly affects hardness.

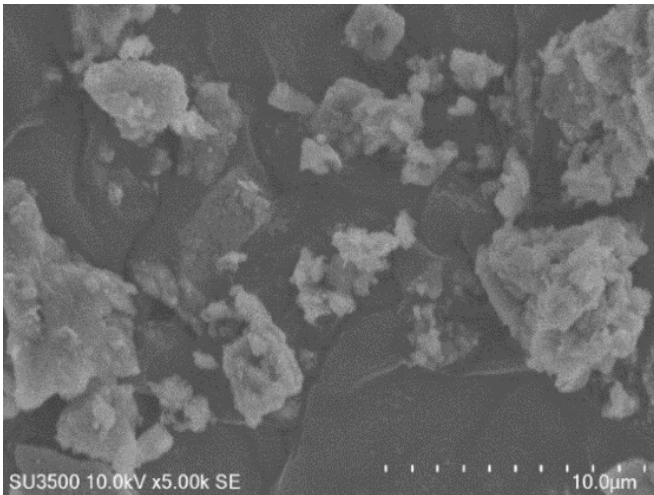


Fig. 7. Microstructure 6 M air cured for 28 days.

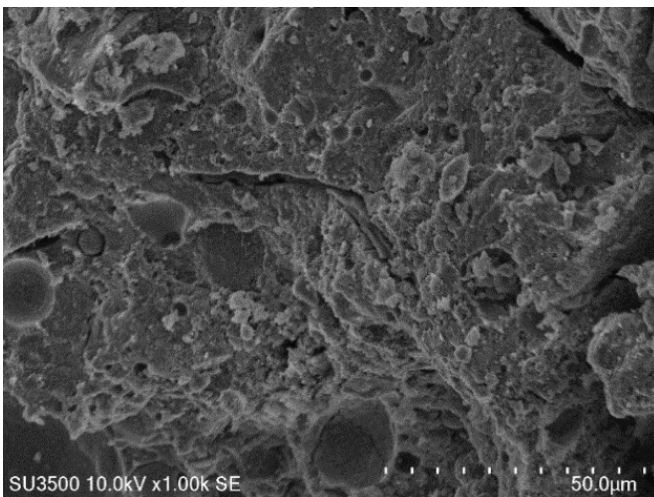


Fig. 8. Microstructure 12 M air cured for 28 days.

Compounds containing silica oxide are essential in identifying a material's level of crystallinity. Calcium silica cement is created when different fine pozzolan components are combined with RSA. FA mostly consists of silica, which when

combined with RSA produces a gel called [Ca(Si)3]. Furthermore, FA has pozzolanic properties, which allow it to combine with RSA, water, and other substances to produce calcium silicate hydrate (C-S-H).

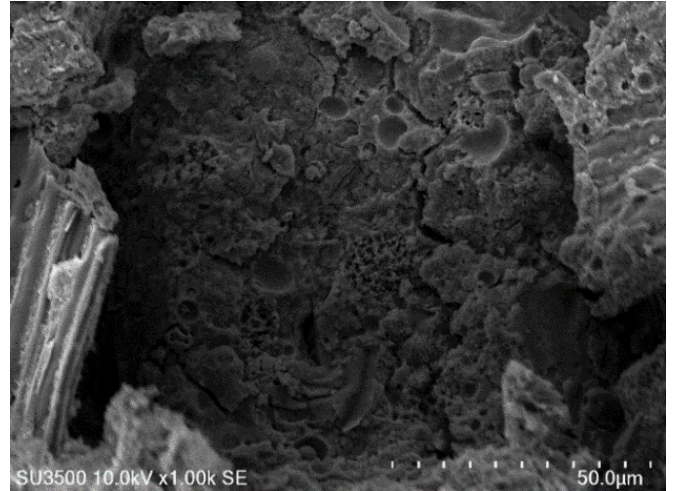


Fig. 9. Microstructure 15 M air cured for 28 days.

The XRD test results showed that, based on the compound content of the mortar's component material, the reaction matched the major compound in the geopolymer mortar. The geopolymer equation used in this work, which includes an alkali activator, FA, RSA, and LS, can be seen in Figure 10. We can show this by using the reaction equation, which is indicated by (1)-(6).

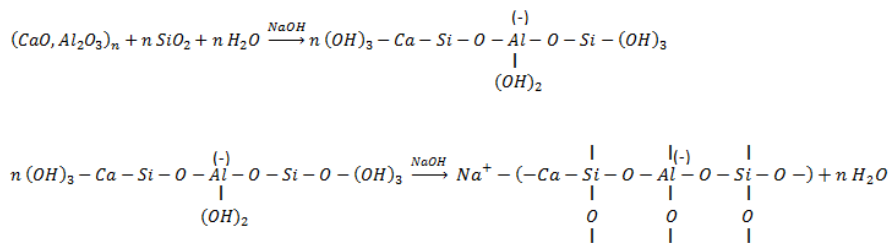
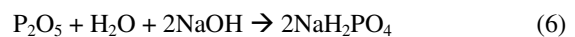
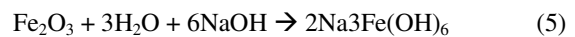
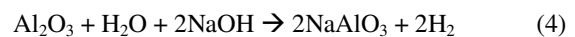
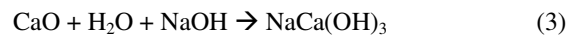
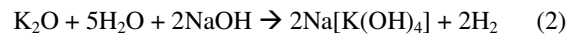
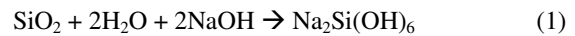


Fig. 10. Geopolymer equation.

Figure 11 shows the results of XRD testing to support the findings obtained from SEM testing (microstructure). There are many chemicals present in the test sample, as indicated by the XRD peaks. The JCPDS (5-0490, 15-0776, 33-0664, 9-351) is

followed, successively, by quartz (Q), mullite (M), hematite (H), and belite (B). Treatments for CA and CU differ in the percentage composition of verified stages, among other things. The stability of the test sample is influenced by the duration of

storage time in both air and water curing treatments, as the figure amply illustrates by the change in intensity value (a.u.). The XRD spectrum's intensity changes will be analyzed to help us comprehend and evaluate the test sample's structural characteristics.

Another technique for analysis that can track alterations in a material's structure at the microscale is the calculation of the degree of crystallinity (%). The Segal calculation method was employed in this work to determine the percentage degree of crystallinity. This calculation involved comparing the recognized crystal peaks with the amorphous background, then multiplying the result by 100 to display the XRD spectra as a percentage. The crystalline spectrum is shown by the blue line in Figure 11, and the amorphous spectrum is represented by the red line. When samples are treated with CA, the orientation of the change in crystallinity value always has a value higher than when samples are treated with air curing.

Changes in crystallinity values in all test samples are influenced by a number of significant factors, two of which are periodicity and atomic arrangement conditions in the test samples (geopolymer materials). The periodicity of the atomic arrangement increases with increasing crystallinity value and vice versa. In order to show how the crystallinity value of a test material affects its compressive strength and how it correlates with the concentration of the compounds that were found, this study made observations. The regularity of the atomic shape of a substance is referred to as its crystal structure. The hardness value of the geopolymer material was manipulated in this investigation by adjusting the molarity concentration of the alkaline activator NaOH. The increase in compressive strength of the geopolymer material indicates that its hardness and density are attributed to the components Fe_3O_4 and SiO_2 .

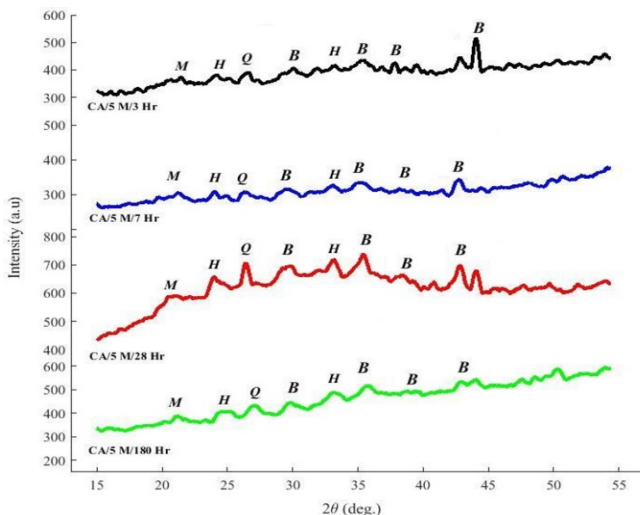


Fig. 11. XRD patterns of geopolymer samples.

IV. CONCLUSION

The purpose of this work is to identify FA, RSA, and LS components as cementitious materials that can be used to replace cement in mortar manufacturing utilizing geopolymer technology. The study concludes with the following findings:

Alumina and amorphous silica can be released by NaOH. Furthermore, without heating, NaOH can be used as a binder for geopolymer mortars made of FA, RSA, and LS. Cement is not required when these components are combined with an alkaline solution to form an alumina-silica binder. Thus, a Si-O-Al polymer link is formed. The test object can harden without needing to be heated in an oven thanks to the occurring polymerization reaction.

The degree of crystallization is crucial in defining the characteristics of the geopolymer material, according to the SEM and XRD data. The compressive strength of the geopolymer is strongly influenced by a certain degree of crystallization.

The findings of this study can offer strong evidence in favor of using waste and locally available ingredients, such as LS and RSA, to make geopolymer mortar. Furthermore, this discovery can help manufacture environmentally friendly (green) materials for national infrastructure development by removing the need for oven heat during the polymerization reaction phase. But because this material is similar to regular concrete, it can also increase the compressive strength of geopolymer mortar.

This study establishes the use of ecologically friendly materials as alternatives to mortar, removing the need for cement and oven heat, as part of sustainable infrastructure development. Emphasis is given on materials that can reduce carbon emissions in their use, and in the reuse of waste resources. The study's findings reveal that when FA, RSA, and LS are coupled with alkaline activators, they form geopolymerization bonds and can be used as mortar materials for plastering with mortar classification B (medium to high strength). As a result, the use of environmentally friendly materials distinguishes this study from others.

ACKNOWLEDGMENT

Both normal and self-compacting concrete specimens were made and conditioned by the Materials and Structural Laboratory at the Department of Civil Engineering, Faculty of Engineering, Christian University of Indonesia, Toraja, Indonesia, in support of this study. The laboratory personnel is much appreciated by the authors for their essential support during this research.

REFERENCES

- [1] P. R. Rangan, M. Tumpu, M. Mansyur, and D. S. Mabui, "Assessment of Fly Ash-Rice Straw Ash-Laterite Soil Based Geopolymer Mortar Durability," *Civil Engineering Journal*, vol. 9, no. 6, pp. 1456–1470, Jun. 2023.
- [2] N. Nurhasmiati, M. F. Samawi, M. Lanuru, P. Taba, F. Fahrudin, and M. Tumpu, "Distribution and Concentration of Pb, Cd, and Hg Metals Due to Land Use Influence on Sediment in Malili River, East Luwu Regency," *Nature Environment and Pollution Technology*, vol. 22, no. 4, pp. 1795–1807, Dec. 2023, <https://doi.org/10.46488/NEPT.2023.v22i04.008>.
- [3] H. Parung, M. Tumpu, M. W. Tjaronge, A. A. Amiruddin, M. A. Walenna, and Mansyur, "Crack Pattern of Lightweight Concrete under Compression and Tensile Test," *Annales de Chimie - Science des Matériaux*, vol. 47, no. 1, pp. 35–41, 2023, <https://doi.org/10.18280/acsm.47i0105>.

- [4] A. Maulana, M. Tumpu, I. P. Indriani, and I. Utama, "Flood Sedimentology for Future Floods Mitigation in North Luwu, Sulawesi, Indonesia," *Civil Engineering Journal*, vol. 9, no. 4, pp. 906–914, Apr. 2023, <https://doi.org/10.28991/CEJ-2023-09-04-011>.
- [5] A. A. Amiruddin, H. Parung, R. Irmawaty, M. Tumpu, Mansyur, and P. R. Rangan, "Ductility and Distribution of Strains on Column Reinforcement Retrofit with Wire Mesh," *Civil and Environmental Engineering*, vol. 19, no. 1, pp. 149–155, May 2023, <https://doi.org/10.2478/cee-2023-0013>.
- [6] P. R. Rangan, M. Tumpu, Y. Sunarno, and M. Mansyur, "Sugarcane bagasse ash-portland composite cement blended in paving blocks production for effective resource utilization between sugar and construction industries," *AIP Conference Proceedings*, vol. 3110, no. 1, Mar. 2024, Art. no. 020025, <https://doi.org/10.1063/5.0205404>.
- [7] P. R. Rangan, M. Tumpu, M. Mansyur, and J. Thoengsal, "A Preliminary Study of Alkali-Activated Pozzolan Materials Produced with Sodium Hydroxide Activator," *International Journal of Engineering Trends and Technology*, vol. 71, no. 6, pp. 375–382, Jul. 2023.
- [8] P. R. Rangan, M. Tumpu, and M. Mansyur, "Study of the effect of soluble silicates (waterglass) and limestone on the compressive strength test, cohesion and modulus of soil stiffness," *AIP Conference Proceedings*, vol. 3110, no. 1, Mar. 2024, Art. no. 020026, <https://doi.org/10.1063/5.0205399>.
- [9] S. H. Mohammed and N. M. Fawzi, "The Effect of the Utilization of Sustainable Materials on Some Mechanical Properties of Geopolymer Mortar," *Engineering, Technology & Applied Science Research*, vol. 14, no. 1, pp. 12464–12469, Feb. 2024, <https://doi.org/10.48084/etasr.6378>.
- [10] M. Tumpu and D. S. Mabui, "Effect of hydrated lime (Ca(OH)₂) to compressive strength of geopolymer concrete," *AIP Conference Proceedings*, vol. 2391, no. 1, Mar. 2022, Art. no. 070011, <https://doi.org/10.1063/5.0086702>.
- [11] Mansyur and M. Tumpu, "Compressive strength of normal concrete using local fine aggregate from Binang River in Bombana district, Indonesia," *AIP Conference Proceedings*, vol. 2391, no. 1, Mar. 2022, Art. no. 070010, <https://doi.org/10.1063/5.0072888>.
- [12] P. R. Rangan, M. Tumpu, and Mansyur, "Marshall Characteristics of Quicklime and Portland Composite Cement (PCC) as Fillers in Asphalt Concrete Binder Course (AC-BC) Mixture," *Annales de Chimie - Science des Matériaux*, vol. 47, no. 1, pp. 51–55, Feb. 2023, <https://doi.org/10.18280/acsm.470107>.
- [13] Mansyur, A. A. Amiruddin, H. Parung, M. W. Tjaronge, and M. Tumpu, "Utilization of Sea Water to Production of Concrete in Terms of Mechanical Behavior," *IOP Conference Series: Earth and Environmental Science*, vol. 921, no. 1, Nov. 2021, Art. no. 012068, <https://doi.org/10.1088/1755-1315/921/1/012068>.
- [14] M. S. Amouri and N. M. Fawzi, "The Effect of Different Curing Temperatures on the Properties of Geopolymer Reinforced with Micro Steel Fibers," *Engineering, Technology & Applied Science Research*, vol. 12, no. 1, pp. 8029–8032, Feb. 2022, <https://doi.org/10.48084/etasr.4629>.
- [15] M. Berra, T. Mangialardi, and A. E. Paolini, "Reuse of woody biomass fly ash in cement-based materials," *Construction and Building Materials*, vol. 76, pp. 286–296, Feb. 2015, <https://doi.org/10.1016/j.conbuildmat.2014.11.052>.
- [16] P. R. Rangan, M. Tumpu, A. T. Arrang, A. Yuniarta, and F. Rachim, "Effect of Curing Time and Liquid Alkaline Activators on Compressive Strength Development of Fly Ash and Bamboo Leaf Ash-Based Geopolymer Concrete," *GEOMATE Journal*, vol. 27, no. 119, pp. 112–119, Jul. 2024.
- [17] M. S. Amouri and N. M. Fawzi, "The Mechanical Properties of Fly Ash and Slag Geopolymer Mortar with Micro Steel Fibers," *Engineering, Technology & Applied Science Research*, vol. 12, no. 2, pp. 8463–8466, Apr. 2022, <https://doi.org/10.48084/etasr.4855>.
- [18] Y. Sunarno, P. R. Rangan, E. Ambun, and M. Tumpu, "Mechanical Properties of Foamed Concrete (FC) Using High-Volume Fly Ash," *GEOMATE Journal*, vol. 26, no. 118, pp. 141–148, Jun. 2024.
- [19] B. Fultz and J. M. Howe, *Transmission Electron Microscopy and Diffractometry of Materials*. New York, NY, USA: Springer, 2012.
- [20] N. W. Gregory, "Elements of X-Ray Diffraction," *Journal of the American Chemical Society*, vol. 79, no. 7, pp. 1773–1774, Apr. 1957, <https://doi.org/10.1021/ja01564a077>.
- [21] P. Chindaprasirt and W. Chalee, "Effect of sodium hydroxide concentration on chloride penetration and steel corrosion of fly ash-based geopolymer concrete under marine site," *Construction and Building Materials*, vol. 63, pp. 303–310, Jul. 2014, <https://doi.org/10.1016/j.conbuildmat.2014.04.010>.
- [22] C. H. Un, J. G. Sanjayan, R. San Nicolas, and J. S. J. van Deventer, "Predictions of long-term deflection of geopolymer concrete beams," *Construction and Building Materials*, vol. 94, pp. 10–19, Sep. 2015, <https://doi.org/10.1016/j.conbuildmat.2015.06.030>.
- [23] A. Mehta and R. Siddique, "Sulfuric acid resistance of fly ash based geopolymer concrete," *Construction and Building Materials*, vol. 146, pp. 136–143, Aug. 2017, <https://doi.org/10.1016/j.conbuildmat.2017.04.077>.
- [24] P. Posi, C. Ridditirud, C. Ekvong, D. Chammanee, K. Janthowong, and P. Chindaprasirt, "Properties of lightweight high calcium fly ash geopolymer concretes containing recycled packaging foam," *Construction and Building Materials*, vol. 94, pp. 408–413, Sep. 2015, <https://doi.org/10.1016/j.conbuildmat.2015.07.080>.
- [25] A. Kumar, Rajkishor, N. Kumar, A. K. Chhotu, and B. Kumar, "Effect of Ground Granulated Blast Slag and Temperature Curing on the Strength of Fly Ash-based Geopolymer Concrete," *Engineering, Technology & Applied Science Research*, vol. 14, no. 2, pp. 13319–13323, Apr. 2024, <https://doi.org/10.48084/etasr.6874>.
- [26] R. Sangi, B. S. Sreenivas, and K. Shanker, "Mix Design of Fly Ash and GGBS based Geopolymer Concrete activated with Water Glass," *Engineering, Technology & Applied Science Research*, vol. 13, no. 5, pp. 11884–11889, Oct. 2023, <https://doi.org/10.48084/etasr.6216>.
- [27] J. Davidovits, "Environmentally Driven Geopolymer Cement Applications," in *Geopolymer 2002 Conference*, Melbourne, Australia, Oct. 2002, pp. 1–9.
- [28] R. H. A. Rahim, T. Rahmiati, K. A. Azizli, Z. Man, M. F. Nuruddin, and L. Ismail, "Comparison of Using NaOH and KOH Activated Fly Ash-Based Geopolymer on the Mechanical Properties," *Materials Science Forum*, vol. 803, pp. 179–184, 2015, <https://doi.org/10.4028/www.scientific.net/MSF.803.179>.
- [29] *ASTM C618-17a(2017), Standard Specification for Coal Fly Ash and Raw or Calcined Natural Pozzolan for Use in Concrete*. West Conshohocken, PA, USA: ASTM International, 2017.
- [30] J. Temuujin, A. van Riessen, and K. J. D. MacKenzie, "Preparation and characterisation of fly ash based geopolymer mortars," *Construction and Building Materials*, vol. 24, no. 10, pp. 1906–1910, Oct. 2010, <https://doi.org/10.1016/j.conbuildmat.2010.04.012>.
- [31] *SNI 1974 (2011), Cara uji kuat tekan beton dengan benda uji silinder*. Jakarta, Indonesia: Standar Nasional Indonesia, 2011.
- [32] *SNI 03-6825 (2002), Metode Pengujian Kekuatan Tekan Mortar Semen*. Jakarta, Indonesia: Standar Nasional Indonesia, 2002.
- [33] P. R. Rangan, R. Irmawaty, M. W. Tjaronge, A. A. Amiruddin, B. Bakri, and M. Tumpu, "The effect of curing on compressive strength of geopolymer mortar made rice straw ash, fly ash, and laterite soil," *IOP Conference Series: Earth and Environmental Science*, vol. 921, no. 1, Nov. 2021, Art. no. 012009, <https://doi.org/10.1088/1755-1315/921/1/012009>.